International Journal of Mass Spectrometry 313 (2012) 30–35

Contents lists available at SciVerse ScienceDirect

International Journal of Mass Spectrometry

journal homepage: www.elsevier.com/locate/ijms

Lifting of the trapping potential during ion storage for multi-anion production in a Penning trap

Franklin Martinez, Steffi Bandelow, Christian Breitenfeldt, Gerrit Marx, Lutz Schweikhard, Frank Wienholtz, Falk Ziegler

Institut für Physik, Ernst-Moritz-Arndt-Universität, 17487 Greifswald, Germany

ARTICLE INFO

Article history:
Received 11 November 2011
Received in revised form
15 December 2011
Accepted 19 December 2011
Available online 28 December 2011

Keywords:
Multiply charged anions
Coulomb barrier
Penning trap
Trapping potential
Electron bath
Aluminum clusters

ABSTRACT

The attempts to produce higher and higher charge states of anionic metal clusters in Penning traps by attachment of simultaneously stored electrons run into a dilemma: On the one hand, the size of the clusters, which are initially only singly charged, has to be increased to accommodate additional electrons. On the other hand, in order to attach to already highly-charged particles, electrons have to overcome the respective Coulomb barriers. Thus, for the conventional electron-bath technique the electrons need to be created at correspondingly higher trapping potentials. This leads to a conflict as the "critical mass", above which the ion orbits are no longer stable, is inversely proportional to the trapping potential. However, as the critical mass is actually an upper limit of the mass-over-charge ratio, the introduction of a stepwise charging-up by repeated electron bathing after increase of the trapping potential allows one to reach higher and higher charge states.

1. Introduction

Multiply negatively charged species in the gas phase have been subject of experimental investigations over the years, and several methods for their production were developed. By sputtering [1], laser ablation [2–4] and electrospray ionization [5,6], doubly-charged anions can be formed in the ion source. Alternatively, mono-anionic species and electrons can be brought together to prompt electron attachment. The latter includes electron transfer reactions [7,8], and direct exposure of trapped mono-anions to an environment of quasi-free electrons, utilizing an electron beam [9,10] or an electron bath [11].

The electron bath uses the capability of Penning ion traps to store electrons and molecular anions, simultaneously. Thus, multiply-charged cluster anions were produced, ranging from di-anionic fullerenes [12,13], gold, silver, copper [11,12,14–17] and titanium [18] cluster di- and tri-anions, to aluminum cluster di-, tri- and tetra-anions [19–22].

On the way to even higher anionic charge states, the conventional electron-bath technique is reaching a limit, as discussed in Section 2. However, by introducing a variation of the trapping potential (Section 3), this limit has been bypassed. Changing the trapping potential during ion storage can be used as a method for the manipulation of the ion motion. This has been utilized, e.g. by adiabatic reduction of the trapping potential for ion cooling in Penning traps [23–25]. In contrast, in the experiments reported here the trapping potential is increased. This allows the creation and storage of electrons with kinetic energies higher than before the increase. As a result, higher charge states of anionic clusters can be produced as shown for the case of aluminum clusters (Section 4).

2. Multi-anion production in a Penning trap

The electron-bath technique for production of multiply charged cluster anions has been developed and applied at the Penning trap setup ClusterTrap [26–29]. In this section, the limitation of the electron-bath technique, caused by two opposing conditions, is discussed. In the first two parts, the Coulomb barrier and resulting trapping requirements for electron attachment to anionic clusters are reviewed. In the third part, the storage limitations of the Penning trap for charged clusters are considered.

2.1. The Coulomb barrier for electron attachment

For the production of multi-anionic cluster species, electrons are sequentially attached to already negatively charged cluster ions, $X_n^z + e^- \rightarrow X_n^{z-1}$. In the charged-metal-sphere model, the electrons

E-mail address: franklin.martinez@physik.uni-greifswald.de (F. Martinez).

1387-3806/$ – see front matter © 2011 Elsevier B.V. All rights reserved.
doi:10.1016/j.ijms.2011.12.009

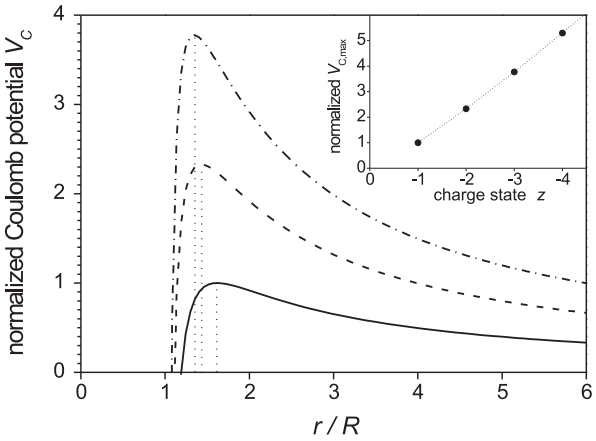

Fig. 1. Normalized Coulomb potential V_C of a cluster anion of radius $R = R(n)$, and charge state z = -1, -2 and -3 (solid, dashed, dash-dotted line, respectively). Inlet: normalized potential maxima $V_{C,max}$ as function of the charge state z.

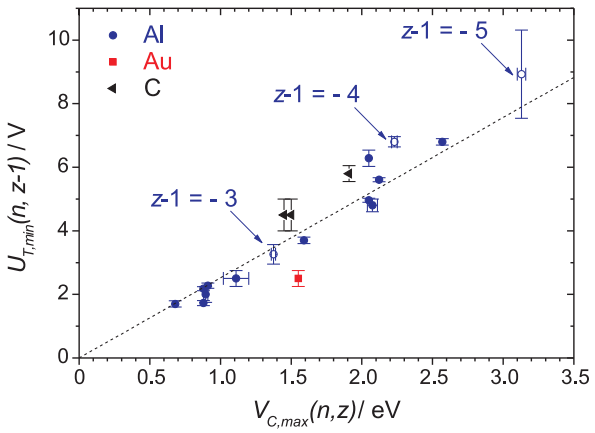

Fig. 2. Experimentally determined minimum trapping potential depths $U_{T,min}$ for production of X_n^{z-1} as function of the numerically calculated[1] Coulomb barrier heights $V_{C,max}$ of the precursor ions X_n^z (X = Al, Au, C). The dashed line is a linear fit through data from [12,13,19,21,22,35] (filled symbols) and zero. Data from present measurements (open symbols, Section 4) are not included in the fit.

have to overcome the repulsive force caused by the Coulomb potential barrier [30] (Fig. 1),

$$V_C(z, r, R) = \frac{e^2}{4\pi\varepsilon_0}\left(\frac{|z|}{r} - \frac{R^3}{2r^2(r^2 - R^2)}\right), \quad (1)$$

of the precursor cluster anion with charge state z and radius $R = R(n)$, given by the number of atoms in the cluster, n. In the following, the radius of a metal cluster is approximated by $R(n) = R_a n^{1/3}$, with R_a being the atomic radius.

The maximum height $V_{C,max}$ of the potential increases with increasing charge state z (Fig. 1, inlet). It determines the minimum energy which is required by an electron to overcome the barrier. Electrons with an energy too low to overcome the barrier are immediately repelled, causing very short interaction times. Thus, tunneling through the Coulomb barrier can be neglected for the process of electron attachment. This is in contrast to the reverse process of electron detachment from multi-anionic clusters: For cluster anions with negative electron affinities, an excess electron might yet be bound by the Coulomb barrier. However, such systems are meta-stable as the electron eventually escapes by tunneling through the barrier [14,16,19,20,22].

2.2. The Penning-trap well depth

The Penning trap consists of a combination of a homogeneous static magnetic field and an electrostatic quadrupolar field, for radial and axial ion confinement, respectively [31–33]. The electric field is generated by the trapping voltage, U_0, applied between a ring and two endcap electrodes. The axial trapping potential well depth

$$U_T = U_0 \frac{z_0^2}{2d_0^2} \quad (2)$$

is given by the geometry factor $d_0^2 = r_0^2/4 + z_0^2/2$, with r_0 and z_0 being the smallest distances of the ring and endcap electrodes to the center of the trap, respectively [12,26,31]. For asymptotically symmetric trap geometries ($z_0^2 = r_0^2/2$), as used at the ClusterTrap experiment, the axial potential well depth is $U_T = U_0/2$ [34].

Previous experimental results show an increase of the relative abundance of multiply charged anions after application of an electron bath as a function of the trapping voltage U_0 [12,13,17,19,21,22,35]. In particular, a minimum potential well depth $U_{T,min} = U_{0,min}/2$ is required to produce a multi-anionic charge state, reflecting the presence of the Coulomb barrier. In Fig. 2 experimentally determined minimum potential well depths $U_{T,min}(n, z-1)$ for the observation of cluster anions X_n^{z-1} (X = Al, Au, C) are plotted against the calculated[1] maxima $V_{C,max}(n, z)$ of the Coulomb barriers of the respective precursor anions, X_n^z (filled symbols). The linear fit to these data points through zero has a slope of $U_{T,min}/V_{C,max} = 2.52(2)$ V/eV. (The points with open symbols are not included in the fit, but are discussed in Section 4.) Fig. 2 shows that for the production of clusters X_n^{z-1}, the potential well depth has to fulfill the condition $U_T \geq U_{T,min}$, with

$$U_{T,min}(n, z-1)[V] \cong 2.5 \cdot V_{C,max}(n, z)[eV], \quad (3)$$

i.e. the trapping voltage $U_0 = 2U_T$ applied at ClusterTrap has to be at least five times higher than the Coulomb-potential maximum of the precursor cluster X_n^z. Eq. (3) can be understood in terms of the energy distribution of the trapped secondary electrons. An upper limit of their axial kinetic energy is given by the potential well depth eU_T. However, this limit is only valid for secondary electrons, that are generated close to the endcap electrodes. Electrons, which are generated closer to the trap center, gain less axial kinetic energy. Consequently, the mean kinetic energy of the trapped electron ensemble is considerably lower than the potential well depth.

2.3. The conflicting requirements for electron attachment to clusters in a Penning trap

Previous investigations of metal cluster (Au, Ag, Cu and Al) and fullerene multi-anions showed, that for the observation of each charge state, a minimum (appearance) cluster size is required [11,13–16,19,20,22]. In other words, to produce higher negative charge states, larger clusters have to be provided. By taking into account the electron affinity, the Coulomb barrier and tunneling effects, the appearance cluster sizes for particular charge states can be estimated [16,20,22,30] based on the charged-sphere model.

Starting point for the multi-anion production are mono-anionic clusters, that are captured in the Penning trap. However, for a given trapping voltage U_0 of the Penning trap, there is an upper limit of the mass-over-charge ratio of trapped ions [37],

$$\left(\frac{m_a n}{|ze|}\right)_{crit} = \frac{d_0^2 B^2}{2U_0}, \quad (4)$$

[1] R_a(Au)=0.159nm [36,12]; R_a(Al)=0.158nm [36]; $R(C_n) = R(C_{60})\sqrt{n/60}$ for n=78 and 84 [13], with $R(C_{60})$=0.42nm [7]; $R(C_{70})$=0.377nm [12].

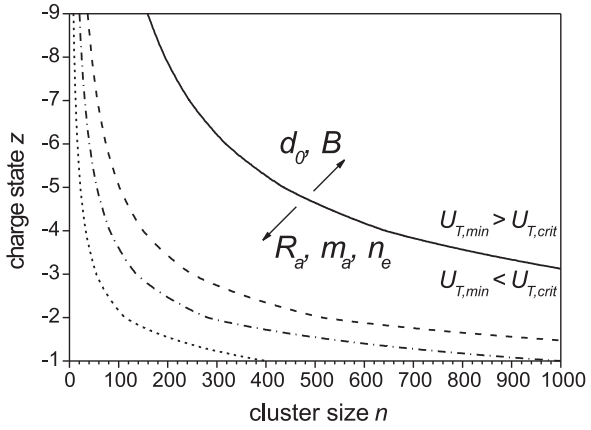

Fig. 3. Maximum charge state z of trapped cluster anions as function of the cluster size n, for which the relation $U_{T,\mathrm{crit}}(n,-1) = U_{T,\mathrm{min}}(n, z-1)$ is fulfilled (Eq. (3), B = 5 T, d_0^2 = 200 mm^2); for aluminum (solid line), copper (dashed line), silver (dash-dotted line) and gold (short-dashed line). As indicated, the curves shift upwards for increasing trap parameters d_0 and B, and downwards for increasing atomic radius R_a, atomic mass m_a and electron density n_e.

where B is the magnetic flux density, and m_a is the atomic mass of the element the cluster consists of. This limit corresponds to an upper limit $U_{0,\mathrm{crit}}$ of the trapping voltage (and potential well depth $U_{T,\mathrm{crit}}$, Eq. (2)) for a trapped cluster of size n and charge state z.

For cluster mono-anions that are stored together with many electrons, the axial trapping potential well depth U_T and the critical trapping voltage $U_{0,\mathrm{crit}}$ are shifted to lower values, as space–charge effects have to be considered. Assuming a space–charge density caused by electrons, $Q_{sc}n_{sc} = en_e$, the well depth and the critical trapping voltage can be estimated by [17,21,38]

$$U_T(n_e) = \frac{U_0 z_0^2}{2d_0^2} - \frac{d_0^2 e n_e}{6\varepsilon_0}, \tag{5}$$

$$U_{0,\mathrm{crit}}(n, z, n_e) = \frac{|ze|d_0^2 B^2}{2m_a n} - \frac{2d_0^2 e n_e}{3\varepsilon_0}. \tag{6}$$

In conclusion, for the production of multi-anionic clusters by application of the electron-bath technique in a Penning trap, two conditions need to be fulfilled: The trapping potential well depth U_T needs to be large enough to allow electron attachment, and at the same time needs to be low enough to store large cluster mono-anions, i.e. $U_{T,\mathrm{min}} < U_T < U_{T,\mathrm{crit}}$. In particular, $U_{T,\mathrm{min}}(n, z-1) < U_{T,\mathrm{crit}}(n, -1)$ must be fulfilled.

Based on this condition, the maximum charge states z of trapped cluster ions for which co-trapped electrons can overcome the Coulomb potential, are shown as a function of the cluster size n in Fig. 3. Note, that in Fig. 3, the stability of multi-anionic clusters, i.e. their size with respect to the appearance cluster size, is not taken into account. Electrons might overcome the Coulomb potential, but may not necessarily be stably bound to the cluster anion.

If one aimes for higher and higher negative charge states, which in turn require an increase of the cluster size, the condition $U_{T,\mathrm{min}} < U_{T,\mathrm{crit}}$ will eventually be violated, with the corresponding charge states and cluster sizes depending on the Penning trap parameters (Eqs. (2), (3) and (6), Fig. 3).

However, there is a solution to this dilemma: The multi-anion production can be performed stepwise, that is, the electron-bath technique has to be modified in such a way, that the trapping voltage U_0 is increased between application of consecutive electron baths. The experimental realization and results of such a procedure are presented in Section 3 and 4.

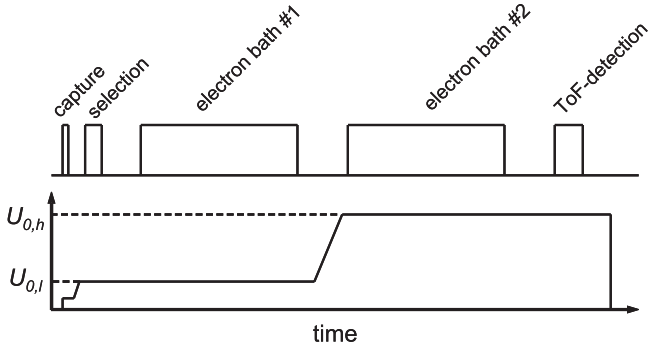

Fig. 4. Experimental sequence of the multi-anion production in the Penning trap. For most effective capture of mono-anions, the trapping voltage is kept at low values at the beginning of the sequence. It is then increased for size selection and application of the first electron bath. Then U_0 is further increased before application of a second electron bath. The product ions are analyzed by time-of-flight mass spectrometry.

3. Experimental setup and procedure

ClusterTrap is a 5-T Penning-trap setup developed for investigations of gas-phase cluster ions [26–29]. Cluster mono-anions are produced in a laser-ablation source [39], accumulated in a radio-frequency ion trap and transferred into the Penning trap. There, the cluster ions are centered by buffer-gas assisted quadrupolar radio-frequency excitation [40,41], size-selected, then subjected to one or several reaction steps, and subsequently the product ions are analyzed by time-of-flight (ToF) mass spectrometry.

The electron-bath [11,20–22] consists of trapped low-energetic secondary electrons, produced in the Penning trap for 200 ms by electron-impact ionization of argon gas. The gas is injected in several pulses from a pulsed leak valve. Each pulse causes a temporary pressure of up to 10^{-5} hPa in the trap, before being pumped away within tens of milliseconds [41]. The primary electron energy is about 110 eV. Variation by ±50 eV shows no significant changes in the experimental results. The subsequent reaction period of the clusters in the electron-bath is typically 1 s.

The procedure is repeated up to three times, for renewal of the electron bath. This renewal is needed due to Coulomb interaction between the electrons, which couples the axial and radial motion, where the latter enhances energy loss by synchrotron radiation [31,12,16,21,27].

In the present experimental scheme (Fig. 4), at the beginning of each cycle the trapping voltage U_0 is kept at 3 V, as capture of large clusters turned out to be most effective at low trapping voltages. For the selection step and the first electron bath U_0 is raised within 10 ms to $U_{0,l}$ = 10 V, and it is then ramped within typically 100 ms to a higher potential $U_{0,h}$, before application of the second electron bath. The variable trapping potential was realized by the output of an arbitrary function generator (SRS DS-345), which was further amplified by a factor of 10 by a voltage amplifier (CGC Instruments). To monitor the initial mono-anion number, a reference cycle was performed alternating with the measurement cycle [28,42]. In this cycle the cluster mono-anions were stored at $U_{0,l}$ = 10 V, without being subjected to the series of electron baths (not shown in Fig. 4).

4. Results

For the production of aluminum cluster anions Al_n^{2-}, Al_n^{3-}, and Al_n^{4-} [19–22] the condition $U_{0,\mathrm{min}}(n, z-1) \leq U_{0,\mathrm{crit}}(n, -1)$ has posed no problem. However, for the production of Al_n^{5-} where the expected required cluster-size range is $n \geq 445$ [43], the available U_0-range becomes critically narrow, as illustrated in Fig. 5. The thin lines indicate critical trapping voltages $U_{0,\mathrm{crit}}$ for aluminum cluster mono- and di-anions, for several electron densities n_e (Eq. (6)).

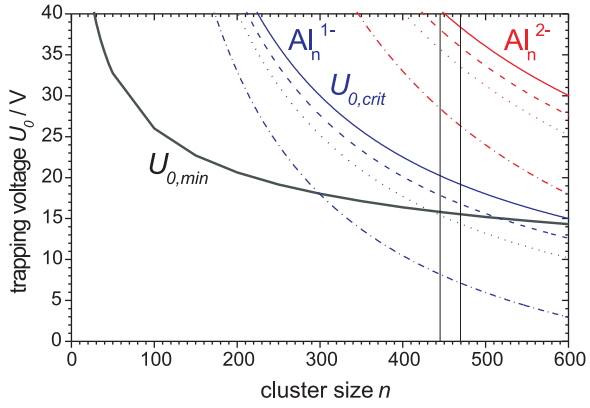

Fig. 5. Critical trapping voltage $U_{0,crit}$ of aluminum cluster mono- and di-anions as a function of the cluster size n, for different electron densities in the Penning trap (0, 1, 2 and 5×10^6 cm^{-3}, thin solid, dashed, dotted and dash-dotted lines, respectively, $B = 5$ T, $d_0^2 = 200$ mm^2). Expected minimum trapping voltage $U_{0,min}$ required for electron attachment to Al_n^{4-} to form Al_n^{5-} (thick solid line). The vertical lines mark the cluster size range, discussed in Section 4.

The thick line represents $U_{0,min}$ as required for electron attachment to Al_n^{4-}, for $n_e = 0$ (Section 2.2). Note, that for $n_e > 0$, the curve for $U_{0,min}$ is shifted upwards to higher voltages, further decreasing the available U_0-range (not shown).

Fig. 6 displays time-of-flight spectra of aluminum cluster anions ($n = 445$–470). The top spectrum shows a reference cycle, where mono-anions are trapped at low $U_{0,l} = 10$ V, without application of any electron bath (Fig. 6a). Due to the limited mass resolving power (≈70) the cluster sizes can not be resolved. While contaminations can not be excluded, nevertheless, bare aluminum clusters are assumed in the following. For the middle spectrum the electron bath has been applied twice at $U_{0,l} = 10$ V (Fig. 6b). Mono-anions remain trapped, but decrease in number, while di- and a few tri-anions appear in the spectrum. The left part of the spectrum is enhanced by a factor of 4, to match the scaling of the spectrum below. There, the trapping voltage has been raised to a high $U_{0,h} = 32$ V for the second electron bath (high-U_0 electron bath, Fig. 6c). Mono-anions leave the trap as their trajectories are unstable above $U_{0,crit} \approx 20$ V (Fig. 5). Di- and tri-anions formed at the $U_{0,l}$ electron bath remain trapped, and some are further converted to tetra- and penta-anions in the $U_{0,h}$ electron bath (Fig. 6c).

The multi-anion production has been investigated as a function of the trapping voltage $U_{0,h}$, making use of three independent

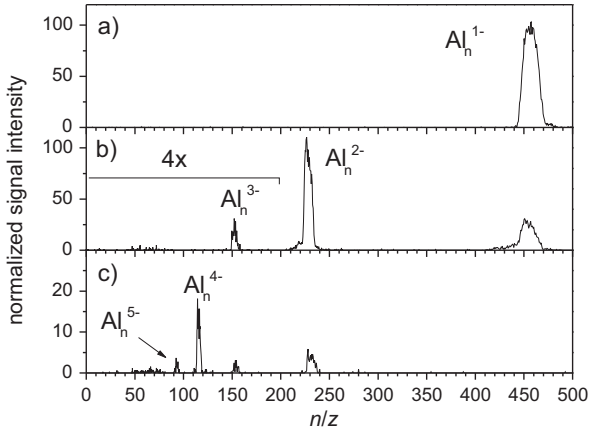

Fig. 6. Time-of-flight spectra of aluminum cluster anions Al_n^z, $n = 445$–470. (a) reference cycle without electron bath, $U_{0,l} = 10$ V, (b) application of two electron baths, both at $U_{0,l} = 10$ V, (c) cycle as in b) but with second electron bath at $U_{0,h} = 32$ V. A part of the spectrum in b) is enhanced to match the scale at c).

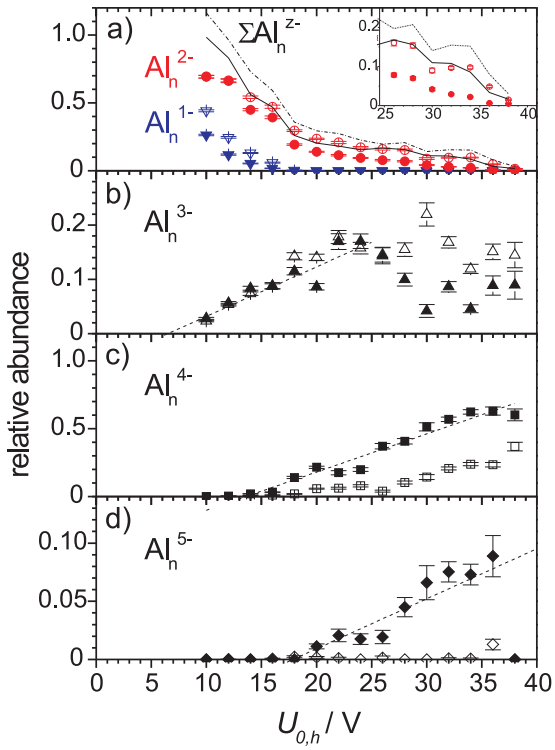

Fig. 7. Relative abundances of negatively charged aluminum clusters ($n = 445$–470) as a function of the trapping voltage $U_{0,h}$. At a first electron bath the trapping voltage was kept at $U_{0,l} = 10$ V, but was varied for a second electron bath, which was applied once (open symbols) and twice (filled symbols). (a) Abundances of Al_n^{1-}, Al_n^{2-} and all product ions Al_n^z (solid and dash-dotted lines) relative to the number of precursor mono-anions. (b–d) Abundances of Al_n^{3-}, Al_n^{4-} and Al_n^{5-}, respectively, relative to the sum of all multiply charged product ions, $\sum Al_n^z$, ($z = -2, \ldots, -5$). The dashed lines are linear fits to the rising edges.

experimental cycles (Fig. 7). The first cycle is the very same as described for Fig. 6c, but with variation of $U_{0,h}$ in the range between 10 and 38 V (open symbols, dashed line in Fig. 7). The second cycle was the same as the first one, except that the $U_{0,h}$ electron bath was applied twice (filled symbols, solid line). The third cycle is a reference cycle without electron bath, as described for Fig. 6a.

Fig. 7a shows the abundance of mono- and di-anions relative to the number of precursor mono-anions from the reference cycle. Additionally, the abundance of the sum of all detected anions ΣAl_n^z ($z = -1, \ldots, -5$) relative to the number of precursor mono-anions is indicated (solid and dashed line). An overall decrease in the total ion number is observed, which is independent of the number of applied electron baths. The decrease is steep up to $U_{0,h} = 18$ V, and than flattens. For the first data point ($U_{0,h} = 10$ V = $U_{0,l}$), where no change of the trapping potential occurs, the abundance of all product ions relative to the number of precursor mono-anions is close to 1 (Fig. 7a, solid and dashed lines). Apparently, the loss of ions is due to the ramping of the trapping potential, rather than to the application of the electron baths.

Most of the ions loss can be understood in terms of the critical mass-over-charge ratio (Section 2.3): The steep part of the decrease is due to the decreasing number of mono-anions; it stops, when the mono-anions fully disappear at $U_{0,h} \cong 18$ V, reaching their trapping limit. Comparison with Fig. 5 indicates an electron density of about $n_e \approx 1 \times 10^6$ cm^{-3}. Above $U_{0,h} = 34$ V, a further decrease is observed, in particular for the cycle with one $U_{0,h}$ electron bath, leading to almost zero in the abundances of all ions at $U_{0,h} = 38$ V (inset Fig. 7a). This again, indicates a trapping limitation, this time for the di-anions, and again at an electron densitiy of $n_e \approx 1 \times 10^6$ cm^{-3} (see

Table 1
Precursor Coulomb-barrier height $V_{C,max}$, experimentally determined minimum trapping voltage $U_{0,min}$, and calculated ratio $U_{T,min}/V_{C,max}$ (using Eq. (5)) of Al_n^z, n = 445–470, for n_e = 0 and 1×10^6 cm^{-3}.

z	$z-1$	$V_{C,max}(z)$ in eV	$U_{0,min}(z-1)$ in V	$U_{T,min}/V_{C,max}$, $n_e = 0$	$U_{T,min}/V_{C,max}$, $n_e = 1 \times 10^6$ cm^{-3}
-2	-3	1.38(2)	6.52(61)	2.37(5)	1.50(5)
-3	-4	2.23(2)	13.60(33)	3.05(1)	2.51(1)
-4	-5	3.13(3)	17.9(2.8)	2.85(20)	2.47(20)

Fig. 5). Electron densities in the same order of magnitude have already been observed at ClusterTrap, earlier [21].

The space charge in the trap might be reduced, and thus the critical trapping potential increased, by removal of the electrons after the first electron bath. As mentioned in Section 3, trapped electrons loose energy over time, and at some point do not contribute to the multi-anion production any longer. If the potential of one or both endcaps is lowered for about 1 μs, the electrons leave the trap, while the slower cluster ions remain trapped (suspended trapping, [44]). Alternatively, axial dipolar radio-frequency excitation is suitable to remove only the electrons from the Penning trap [21].

Fig. 7b–d shows the abundances of product ions Al_n^{3-}, Al_n^{4-} and Al_n^{5-}, respectively, relative to the number of all multiply charged product ions, $\sum Al_n^z$, $z = -2, \ldots, -5$. Up to $U_{0,h} \cong 14$ V, only di- (Fig. 7a) and tri-anions are observed, showing about the same relative ratios after one (open symbols) and two $U_{0,h}$ electron baths (filled symbols). Above $U_{0,h} \cong 14$ V, tetra-anions are formed, and in this range, the repeated application of the $U_{0,h}$ electron bath effects also the relative abundances, reducing the amount of di- and tri-anions, and increasing the number of tetra-anions, as compared to single application. Above $U_{0,h} \cong 18$ V, penta-anions appear, but only after two applications of the $U_{0,h}$ electron bath.

The multi-anion distributions are dominated by di-anions up to $U_{0,h}$ = 25 V, and by tetra-anions for higher trapping voltages (see also Fig. 6). The tri-anion abundance is strikingly low (note the different scales in Fig. 7b–d), even for low $U_{0,h}$, where no tetra-anions are formed, yet. In contrast, for some measurements (spectra not shown) with two $U_{0,h}$ electron baths no penta-anions are observed, while at the same time, the tri-anion abundance is comparable to the tetra-anion abundance. There is as yet no explanation for this observation.

The considerable ion loss (i.e. from 70 down to 10% for the di-anions, Fig. 7a) is affecting the total multi-anion yield. While the penta-anion yield relative to all multi-anions is about 7% in the range $U_{0,h}$ = 30 to 34 V (Fig. 7d), the total multi-anion yield is only 10% relative to the initial mono-anion number (Fig. 7a). This results in a total penta-anion yield of 0.7% with respect to the initial mono-anion number. At about 300 mono-anions per experimental cycle, this results in only 2 penta-anions detected per cycle. Centering of the ions before ramping, and a slower ramping rate might reduce the ion loss in future experiments.

Minimum trapping voltages $U_{0,min}$ have been determined from linear fits (dashed lines in Fig. 7b–d), and are given in Table 1. They increase with the charge state, again reflecting the increasing height of the Coulomb barrier (Fig. 1, Table 1). For calculation of the respective ratios $U_{T,min}/V_{C,max}$, the space–charge effect of the electron cloud at the corresponding trapping potential well depth $U_{T,min}$ should be taken into account (Eq. (5)). For the data presented here, the electron density is estimated from the shift of the critical trapping voltage $U_{0,crit}$ (Fig. 5), to be $n_e \approx 1 \times 10^6$ cm^{-3}. Its consideration for the calculation of U_T results in ratios $U_{T,min}/V_{C,max}$ as presented in Table 1. But, as no electron densities were known for the data in Fig. 2 (filled symbols), those potential well depths U_T were calculated according to Eq. (2). For comparison, the ratios for n_e = 0 from Table 1 have been added to the data points in Fig. 2 (open symbols). While the ratio for the production of tri-anions and penta-anions is in agreement with the expected value of 2.52(2) V/eV (Section 2.2), the ratio of the tetra-anions is somewhat higher. However, it is still within the scattering of the previous data. This scattering is probably due to variations of the electron bath parameters in the different measurements, in particular the poorly known electron density.

5. Conclusion

The production of multi-anionic metal clusters in a Penning trap by the electron-bath method has been investigated with respect to the trapping voltage U_0. Analysis of previous measurements suggest that at ClusterTrap a minimum trapping voltage of at least five times the height of the Coulomb barrier potential of an anionic cluster is required for the attachment of a further electron. In the case of aluminum clusters the minimum trapping potential, required for production of Al_n^{5-}, is similar to the upper limit of the trapping potential for the cluster sizes required for production of penta-anions.

This conflict has been solved by increasing the trapping potential between two electron baths while the cluster ions have been kept stored. Thus, penta-anionic clusters $Al_{445-470}^{5-}$ have been produced, and minimum trapping voltages $U_{0,min}$ for the production of tri-, tetra- and penta-anions have been determined. The respective ratios $U_{T,min}/V_{C,max}$ follow the trend of previous measurements.

Besides supporting the production of multi-anionic species, increasing of the trapping voltage might be a useful technique for selection of high charge states. The critical trapping potential is inversely proportional to the mass-over-charge ratio. Thus lower charge states of a given cluster size can be removed from the trap by raising the trapping potential.

Acknowledgments

The project was supported by a Collaborative Research Center of the DFG (SFB 652-TP A03). F. Martinez and S. Bandelow have received postgraduate stipends from the state of Mecklenburg-Vorpommern (Landesgraduiertenförderung) in the framework of the International Max Planck Research School on Bounded Plasmas.

Appendix A.

The potential maximum $V_{C,max}$ of the Coulomb barrier is calculated from its relative position $r_{C,max}/R$, by use of Eq. (1). While for $z = -1$, the relative maximum position can be calculated analytically, resulting in the golden ratio $(\sqrt{5}+1)/2 = 1 + (\sqrt{5}-1)/2$ [14], for higher charge states, $z = -2, -3, \ldots$, numerical calculations are required.

For an estimation of $V_{C,max}$, the numerically calculated maximum position (Fig. 8a, open squares) has been fitted as a function of the charge state z by

$$\frac{r_{C,max}}{R}(z) = 1 + \frac{\sqrt{5}-1}{2} \cdot |z|^{\alpha}, \tag{7}$$

(solid line). The only free fit parameter α has been determined from the range $z = -1, \ldots, -9$, yielding the value $\alpha = -0.5378(8)$. In Fig. 8b the relative deviation of the fit function (Eq. (7)) from the

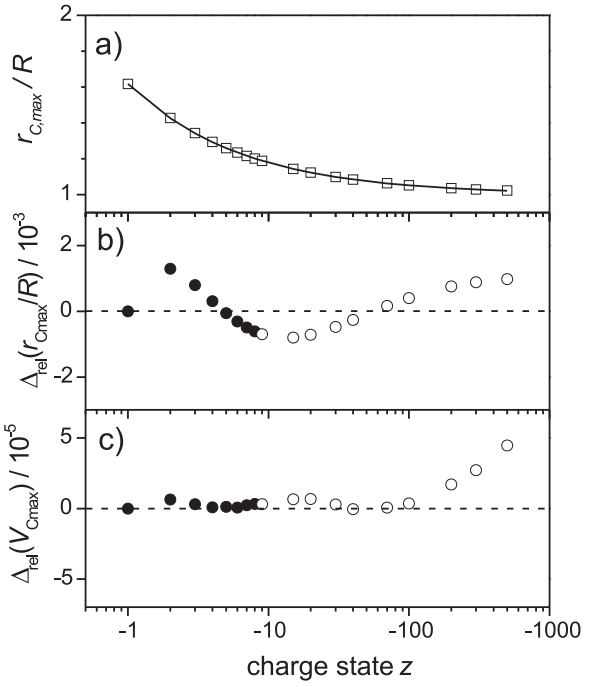

Fig. 8. (a) Relative position $r_{C,max}/R$ of the Coulomb potential maximum $V_{C,max}$ as calculated numerically from Eq. (1) (open squares), and fitted with Eq. (7) (solid line) for $z = -1, \ldots, -9$. (b) Relative deviation of the fitted function for $r_{C,max}/R$ and (c) for $V_{C,max}$. (b) and (c): filled symbols for fitted data, open symbols for extrapolated data.

numerically determined values for $r_{C,max}/R$ is plotted. The correspondingly approximated values for $V_{C,max}$ (Eqs. (1) and (7)) deviate from the numerical values by less than 1×10^{-5} even beyond the fitted range (filled circles) up to $z = -100$ (Fig. 8c, open circles, note the logarithmic scaling).

References

[1] S.N. Schauer, P. Williams, R.N. Compton, Phys. Rev. Lett. 65 (1990) 625.
[2] P.A. Limbach, L. Schweikhard, K.A. Cowen, M.T. McDermott, A.G. Marshall, J.V. Coe, J. Am. Chem. Soc. 113 (1991) 6795.
[3] R.L. Hettich, R.N. Compton, R.H. Ritchie, Phys. Rev. Lett. 67 (1991) 1242.
[4] C. Stoermer, J. Friedrich, M.M. Kappes, Int. J. Mass Spectrom. 206 (2001) 63.
[5] X.-B. Wang, L.S. Wang, W.R. Wiley, Phys. Rev. Lett. 83 (1999) 3402.
[6] O. Hampe, M. Neumaier, M.N. Blom, M.M. Kappes, Chem. Phys. Lett. 354 (2002) 303.
[7] B. Liu, P. Hvelplund, S. Brøndsted Nielsen, S. Tomita, Phys. Rev. Lett. 92 (2004) 168301.
[8] P. Hvelplund, B. Liu, S. Brøndsted Nielsen, S. Tomita, Eur. Phys. J. D 43 (2007) 133.
[9] K. Leiter, W. Ritter, A. Stamatovic, T.D. Märk, Int. J. Mass Spectrom. Ion Process. 68 (1986) 341.
[10] J. Hartig, M.N. Blom, O. Hampe, M.M. Kappes, Int. J. Mass Spectrom. 229 (2003) 93.
[11] A. Herlert, S. Krückeberg, L. Schweikhard, M. Vogel, C. Walther, Phys. Scr. T 80 (1999) 200.
[12] A. Herlert, R. Jertz, J. Alonso Otamendi, A.J. Gonzalez Martinez, L. Schweikhard, Int. J. Mass Spectrom. 218 (2002) 217.
[13] A. Lassesson, N. Walsh, F. Martinez, A. Herlert, G. Marx, L. Schweikhard, Eur. Phys. J. D 34 (2005) 73.
[14] L. Schweikhard, A. Herlert, S. Krückeberg, M. Vogel, C. Walther, Philos. Mag. B 79 (1999) 1343.
[15] A. Herlert, L. Schweikhard, M. Vogel, Eur. J. Phys. D 16 (2001) 65.
[16] A. Herlert, L. Schweikhard, Int. J. Mass Spectrom. 229 (2003) 19.
[17] L. Schweikhard, A. Herlert, G. Marx, AIP Conf. Proc. 692 (2003) 203.
[18] A. Herlert, K. Hansen, L. Schweikhard, M. Vogel, Hyperfine Interactions 127 (2000) 529.
[19] N. Walsh, F. Martinez, G. Marx, L. Schweikhard, Eur. Phys. J. D 43 (2007) 241.
[20] N. Walsh, F. Martinez, G. Marx, L. Schweikhard, F. Ziegler, Eur. Phys. J. D 52 (2009) 27.
[21] N. Walsh, A. Herlert, F. Martinez, G. Marx, L. Schweikhard, J. Phys. B 42 (2009) 154024.
[22] N. Walsh, F. Martinez, G. Marx, L. Schweikhard, F. Ziegler, J. Chem. Phys. 132 (2010) 014308.
[23] S.L. Rolston, G. Gabrielse, Hyperfine Interactions 44 (1988) 233.
[24] G.-Z. Li, R. Poggiani, G. Testera, G. Werth, Z. Phys. D 22 (1991) 375.
[25] G.-Z. Li, R. Poggiani, G. Testera, G. Werth, Hyperfine Interactions 76 (1993) 281.
[26] S. Becker, K. Dasgupta, G. Dietrich, H.J. Kluge, S. Kuznetsov, M. Lindinger, K. Lützenkirchen, L. Schweikhard, J. Ziegler, Rev. Sci. Instrum. 66 (1995) 4902.
[27] L. Schweikhard, K. Hansen, A. Herlert, G. Marx, M. Vogel, Eur. Phys. J. D 24 (2003) 137.
[28] L. Schweikhard, S. Becker, K. Dasgupta, et al., Phys. Scripta T59 (1995) 236.
[29] F. Martinez, G. Marx, L. Schweikhard, A. Vass, F. Ziegler, Eur. Phys. J. D 63 (2011) 255.
[30] J.D. Jackson, Classical Electrodynamics, 3rd ed., Wiley, New York, USA, 1998.
[31] L.S. Brown, G. Gabrielse, Rev. Mod. Phys. 58 (1986) 233.
[32] P.K. Gosh, Ion traps, Oxford University Press, Oxford UK, 1995.
[33] F.G. Major, V.N. Gheorghe, G. Werth, Charged Particle Traps, Springer Verlag, New York, USA, 2005.
[34] R.D. Knight, Int. J. Mass Spectrom. Ion Phys. 51 (1983) 127.
[35] N. Walsh, Multiply-negatively charged aluminium clusters and fullerenes, PhD thesis, Greifswald, Germany (2008).
[36] Ch. Kittel, Einführung in die Festkörperphysik, 14th ed., Oldenbourg Wissenschaftsverlag, London UK, 1994.
[37] L. Schweikhard, J. Ziegler, H. Bopp, K. Lützenkirchen, Int. J. Mass Spectrom. Ion Process. 141 (1995) 77.
[38] J.B. Jeffries, S.E. Barlow, G.H. Dunn, Int. J. Mass Spectrom. Ion Processes 54 (1983) 169–187.
[39] R. Weidele, U. Frenzel, T. Leisner, D. Kreisle, Z. Phys. D 20 (1991) 411.
[40] G. Savard, St. Becker, G. Bollen, H.-J. Kluge, R.B. Moore, Th. Otto, L. Schweikhard, H. Stolzenberg, U. Wiess, Phys. Lett. A 158 (1991) 247.
[41] H.-U. Hasse, St. Becker, G. Dietrich, N. Klisch, H.-J. Kluge, M. Lindinger, K. Lützenkirchen, L. Schweikhard, J. Ziegler, Int. J. Mass Spectrom. 132 (1994) 181.
[42] F. Ziegler, D. Beck, H. Brand, H. Hahn, G. Marx, L. Schweikhard, submitted for publication.
[43] F. Martinez, S. Bandelow, C. Breitenfeldt, G. Marx, L. Schweikhard, F. Wienholtz, F. Ziegler, in preparation.
[44] D.A. Laude, S.C. Beu, Anal. Chem. 61 (1989) 2422.